doi:10.1093/brain/awm336 *Brain* (2008), **131**, 665–680

^{11}C PiB and structural MRI provide complementary information in imaging of Alzheimer's disease and amnestic mild cognitive impairment

Clifford R. Jack, Jr,[1] Val J. Lowe,[1] Matthew L. Senjem,[2] Stephen D. Weigand,[3] Bradley J. Kemp,[1] Maria M. Shiung,[1] David S. Knopman,[4] Bradley F. Boeve,[4] William E. Klunk,[5] Chester A. Mathis[5] and Ronald C. Petersen[4]

[1]Department of Diagnostic Radiology, [2]Information Services, [3]Division of Biostatistics, [4]Neurology Mayo Clinic and Foundation, Rochester, MN and [5]University of Pittsburgh School of Medicine Pittsburgh, PA, USA

Correspondence to: Clifford R. Jack, Jr, MD, Mayo Clinic, Diagnostic Radiology, 200 First Street SW, Rochester, MN 55905, USA.
E-mail: jack.clifford@mayo.edu

To date, most diagnostic imaging comparisons between amyloid labelling ligands and other imaging modalities have been between the use of amyloid labelling ligand ^{11}C Pittsburgh Compound B (PiB) and FDG-PET. Our objectives were to compare cognitive performance and diagnostic group-wise discrimination between cognitively normal, amnestic mild cognitive impairment (MCI) and Alzheimer's disease subjects with MRI-based measures of hippocampal volume and PiB retention, and secondly to evaluate the topographic distribution of PiB retention and grey matter loss using 3D voxel-wise methods. Twenty cognitively normal, 17 amnestic MCI and 8 probable Alzheimer's disease subjects were imaged with both MRI and PiB. PiB retention was quantified as the ratio of uptake in cortical to cerebellar regions of interest (ROIs) 40–60 min post-injection. A global cortical PiB retention summary measure was derived from six cortical ROIs. Statistical parametric mapping (SPM) and voxel-based morphometry (VBM) were used to evaluate PiB retention and grey matter loss on a 3D voxel-wise basis. Alzheimer's disease subjects had high global cortical PiB retention and low hippocampal volume; most cognitively normal subjects had low PiB retention and high hippocampal volume; and on average amnestic MCI subjects were intermediate on both PiB and hippocampal volume. A target-to-cerebellar ratio of 1.5 was used to designate subjects with high or low PiB cortical retention. All Alzheimer's disease subjects fell above this ratio, as did 6 out of 20 cognitively normal subjects and 9 out of 17 MCI subjects, indicating bi-modal PiB retention in the latter two groups. Interestingly, we found no consistent differences in learning and memory performance between high versus low PiB cognitively normal or amnestic MCI subjects. The SPM/VBM voxel-wise comparisons of Alzheimer's disease versus cognitively normal subjects provided complementary information in that clear and meaningful similarities and differences in topographical distribution of amyloid deposition and grey matter loss were shown. The frontal lobes had high PiB retention with little grey matter loss, anteromedial temporal areas had low PiB retention with significant grey matter loss, whereas lateral temporoparietal association cortex displayed both significant PiB retention and grey matter loss. A voxel-wise SPM conjunction analysis revealed that subjects with high PiB retention shared a common PiB retention topographical pattern regardless of clinical category, and this matched that of amyloid plaque distribution from autopsy studies of Alzheimer's disease. Both global cortical PiB retention and hippocampal volumes demonstrated significant correlation in the expected direction with cognitive testing performance; however, correlations were stronger with MRI than PiB. Pair-wise inter-group diagnostic separation was significant for all group-wise pairs for both PiB and hippocampal volume with the exception of the comparison of cognitively normal versus amnestic MCI, which was not significant for PiB. PiB and MRI provided complementary information such that clinical diagnostic classification using both methods was superior to using either in isolation.

Keywords: Alzheimer's disease; mild cognitive impairment; Pittsburgh Compound B; amyloid imaging; magnetic resonance imaging; hippocampus

Abbreviations: AD = Alzheimer's disease; aMCI = amnestic mild cognitive impairment; AVLT = auditory verbal learning test; CDR-SB = Clinical Dementia Rating scale – sum of boxes; CN = cognitively normal; MMSE = Mini Mental State Exam; PiB = ^{11}C Pittsburgh Compound; ROI = region of interest; SPM = statistical parametric mapping; STMS = Short Test of Mental Status; TPM = tissue probability maps; VBM = voxel-based morphometry; WMS-R = Wechsler Memory Scale-Revised

Received August 31, 2007. Revised November 21, 2007. Accepted December 19, 2007. Advance Access publication February 7, 2008

Introduction

The pathological hallmarks of Alzheimer's disease (AD) are amyloid plaques and neurofibrillary tangles. Other associated pathological changes are loss of neurons, loss of synapses and dendritic dearborization. Although these latter neuronal changes are less amenable to assessment by standard pathological techniques, neuronal changes, particularly synapse loss, have been identified as the most proximate histological substrate of the observed clinical symptoms in this disease (Terry *et al.*, 1991).

The most significant advance in dementia imaging in recent years has been the development of *in vivo* amyloid plaque labelling compounds (Klunk *et al.*, 2004; Verhoeff *et al.*, 2004; Small *et al.*, 2006). The most widely studied *in vivo* amyloid labelling tracer at this point is the PET ligand {*N*-methyl-^{11}C}2-(4′-methylaminophenyl)-6-hydroxybenzothiazole also know as Pittsburgh Compound B or PiB (Klunk *et al.*, 2004). *In vivo* PiB studies demonstrate a roughly 2-fold increase in tracer retention in AD patients compared to most cognitively normal elderly subjects (Klunk *et al.*, 2004). Moreover, the topographical distribution of PiB retention matches that expected on the basis of autopsy studies of regional fibrillar plaque distribution (Braak and Braak, 1991; Rowe *et al.*, 2007). Greatest retention values are seen in prefrontal and lateral temporoparietal cortex, posterior cingulate/precuneus and striatum (Klunk *et al.*, 2004; Engler *et al.*, 2006; Kemppainen *et al.*, 2006; Mintun *et al.*, 2006; Edison *et al.*, 2007; Forsberg *et al.*, 2007). Occipital lobe and thalamus display lower uptake values. The lowest uptake values are seen in the medial temporal lobe and primary visual and sensory motor cortical areas. In short, the topographical pattern of PiB binding corresponds to Braak and Braak plaque stage C in most cases of clinically established AD (Braak and Braak, 1991; Rowe *et al.*, 2007). PiB binds to fibrillar amyloid primarily in neuritic and diffuse plaques although in the only imaging-autopsy study published to date, PiB binding correlated to both plaques and vascular amyloid (amyloid angiopathy) (Bacskai *et al.*, 2007). Uptake in cerebellar grey matter does not differ between AD and cognitively normal (CN) subjects as would be predicted because few, if any, fibrillar plaques are typically found in the diseased cerebellum at autopsy (Rowe *et al.*, 2007). Nearly all clinically diagnosed AD subjects reported to date show PiB retention, while the majority of CN do not. However, ~30% of the latter demonstrate amyloid retention levels in cortex which are in the typical range for AD (Mintun *et al.*, 2006). This is consistent with autopsy studies which find pathology consistent with a pathological diagnosis of AD in up to 30% of clinically asymptomatic subjects (Katzman *et al.*, 1988; Crystal *et al.*, 1993; Hulette and Welsh-Bohmer, 1998; Price and Morris, 1999; Schmitt *et al.*, 2000; Morris and Price, 2001; Riley *et al.*, 2002; Knopman *et al.*, 2003). PiB studies which have included patients with amnestic mild cognitive impairment (aMCI) typically find that on average this group lies in an intermediate position between CN and AD subjects. However, approximately two-thirds of them cluster in the AD range with a topographical PiB distribution pattern that is indistinguishable from AD, while one-third cluster in the CN range (Lopresti *et al.*, 2005; Kemppainen *et al.*, 2007; Rowe *et al.*, 2007). Cortical PiB and CSF amyloid beta 42 levels are inversely correlated in both demented and non-demented subjects (Fagan *et al.*, 2006). Cortical PiB binding is typically present in patients with dementia with Lewy bodies, but at lower levels than in patients with AD (Rowe *et al.*, 2007). PiB binding is absent in the majority of clinically diagnosed patients with frontotemporal dementia and when present could represent either coexistent AD and frontal temporal lobe dementia pathology or clinical misdiagnosis (Rabinovici *et al.*, 2007; Rowe *et al.*, 2007). Strong spatial correlation exists between the topography of PiB deposition and default mode functional MRI patterns (Buckner *et al.*, 2005). Rates of brain atrophy from serial MRI studies are greater in AD patients with higher PiB retention (Archer *et al.*, 2006).

Structural MRI has been employed to study AD for over a decade and a half. The initial studies aimed at early diagnosis focused on medial temporal lobe anatomy, particularly the hippocampus, due to the well-established topographical progression of neurofibrillary pathology which begins in the medial temporal lobe structures and progresses from there to paralimbic, basal temporal and other neocortical association areas (de Leon *et al.*, 1989; Braak and Braak, 1991; Jack *et al.*, 1992; Killiany *et al.*, 1993; Laakso *et al.*, 1998). Hippocampal volumes measured from ante-mortem MRI scans correlate with Braak neurofibrillary tangle pathological staging in both demented and non-demented subjects (Gosche *et al.*, 2002; Jack *et al.*, 2002). Ante-mortem hippocampal volume from MRI correlates with hippocampal neurofibrillary tangle density (Silbert *et al.*, 2003; Csernansky *et al.*, 2004) at autopsy and ante-mortem brain volume on MRI correlates with hippocampal plaque density (Csernansky *et al.*, 2004). Ante-mortem rates of brain atrophy correlate with neurofibrillary tangle density and rates of ventricular

expansion correlate with both plaque and tangle density at autopsy (Silbert *et al.*, 2003). Excellent correlation is found between hippocampal volume measures obtained on either ante-mortem MRI (Zarow *et al.*, 2005) or post-mortem MRI (Bobinski *et al.*, 2000) and hippocampal neuron cell counts in autopsy specimens. On the basis of these imaging-to-pathological correlation studies, quantitative measures from structural MRI, such as hippocampal volume, are inferred to represent an approximate surrogate of the stage/severity of neuronal pathology – neuron loss, neuron shrinkage and synapse loss – that occur in AD. Voxel-wise studies of grey matter loss in both AD and aMCI demonstrate that the topographical distribution of grey matter loss closely mirrors the spatial distribution of neurofibrillary pathology described by Braak and Braak (Rombouts *et al.*, 2000; Baron *et al.*, 2001; Chetelat *et al.*, 2002; Frisoni *et al.*, 2002; Senjem *et al.*, 2005; Whitwell *et al.*, 2007*a*, *b*).

To date, most diagnostic imaging comparisons between amyloid labelling ligands and other imaging modalities have been between PiB and FDG-PET (Engler *et al.*, 2006; Edison *et al.*, 2007; Forsberg *et al.*, 2007). Our objectives in the present study were 2-fold. First, to compare cognitive performance and diagnostic group-wise discrimination in CN, aMCI and AD subjects with MRI-based measures of hippocampal volume and PiB retention. Our second objective was to evaluate the topographical distribution of PiB retention and grey matter loss using 3D voxel-wise methods.

Methods

Subjects

All subjects were recruited from the Mayo Alzheimer's Disease Research Center (ADRC) or Alzheimer's Disease Patient Registry (ADPR) (Petersen *et al.*, 1990). These are longitudinal studies of aging and dementia which include serial MRI, clinical and cognitive assessments. At baseline, all subjects met criteria for CN or aMCI or AD. Categorization into diagnostic groups was made on a clinical basis at consensus conferences including neurologists, neuropsychologists, a neuropsychiatrist and study coordinators. CN subjects were asymptomatic cognitively normal volunteers. Criteria for the categorization of CN were: (i) no active neurological or psychiatric disorders; (ii) some subjects may have had ongoing medical problems, yet the illnesses or their treatments did not interfere with cognitive function; (iii) normal neurological exam; and (iv) were independently functioning community dwellers. Criteria for the diagnosis of aMCI were those of Petersen *et al.* (2001): (i) memory complaint documented by the patient and collateral source; (ii) relatively normal general cognition; (iii) normal activities of daily living; (iv) not demented (DSM-IV); and (v) memory impaired for age and education. In general, the aMCI determination is made when the memory measures fall –1.0 to –1.5 SD below the means for age and education appropriate individuals in our community. Rigid cut-offs on psychometric scores were however not used to establish the diagnosis of aMCI which was made on clinical grounds. The diagnosis of dementia was made using DSM-IV criteria (1994), and the diagnosis of AD was made using established criteria (McKhann *et al.*, 1984). The Clinical Dementia Rating scale – sum of boxes (CDR-SB) was used to assess functional performance (Morris, 1993). A 38-item test, the Short Test of Mental Status (STMS) (Kokmen *et al.*, 1991), was used to assess global cognitive performance. Because this test, while sensitive to differences between CN and MCI, is not widely used, we converted STMS scores to Mini Mental State Exam (MMSE) (Folstein *et al.*, 1975) scores using an algorithm developed at our centre (Tang-Wai *et al.*, 2003). STMS values transformed to MMSE scores are reported as MMSE* throughout the manuscript. Learning and memory performance was assessed with the Wechsler Memory Scale-Revised (WMS-R) visual reproduction II, WMS-R logical memory II, Auditory Verbal Learning test (AVLT) delayed recall and AVLT sum of learning trials 1–5 (Rey, 1964; Wechsler, 1987).

The ADPR and ADRC studies have included serial MRI examinations for a number of years. The capacity to perform PiB studies at our institution was brought online within the past year. Subjects included in this study represent all CN, aMCI and AD subjects recruited to date (20 CN, 17 aMCI and 8 AD) who volunteered to participate in both MRI and PiB. No other criteria were used to select the subjects in this analysis. One potential AD subject that did undergo PiB imaging was excluded from this analysis because of elevated PiB retention in cerebellar cortex. In the absence of an accepted physiological explanation, this unexpected finding is under independent investigation.

MRI methods

All MRI studies were performed with a standardized imaging protocol. Forty-one of these subjects were imaged at 3T with a 3D magnetization prepared rapid acquisition gradient echo (MPRAGE) imaging sequence developed for the Alzheimer's Disease Neuroimaging Initiative study (Jack *et al.*, 2007). Parameters were: TR/TE/T1, 2300/3/900 ms; flip angle 8°, 26-cm field of view (FOV); 256 × 256 in-plane matrix with a phase FOV of 0.94, and slice thickness of 1.2 mm. Four subjects were studied at 1.5 T with a coronal volumetric SPGR sequence: 124 contiguous partitions, 1.6-mm slice thickness, 24×18.5-cm FOV, minimum full TE, TR 23 ms and 25° flip angle. All scanners undergo a standardized quality control calibration procedure every morning, which monitors geometric fidelity over a 200-mm volume along all three cardinal axes, signal-to-noise ratio and transmit gain.

All scans underwent correction for gradient non-linearity (gradwarp) and intensity non-uniformity (Jack *et al.*, 2007). MRI processing steps were performed by a research technician (M.M.S.) who was blinded to all clinical information. The borders of the left and right hippocampi were traced sequentially from posterior to anterior using anatomic landmarks that have been previously published (Jack *et al.*, 1989). Test–re-test reproducibility expressed as coefficient of variation for hippocampal volume measurements has been previously measured at 0.28% (Jack *et al.*, 1998). Because four subjects were scanned at 1.5 T, we performed internal quality assurance testing comparing hippocampal tracing results in 10 healthy elderly volunteer subjects who underwent MRI exams at both 1.5 T and 3 T on the same day. The median hippocampal volume difference between the two field strengths was 3.3 mm^3 (or 0.1%). The intra-class correlation between hippocampal volume measurements at the two field strengths was 0.99. Therefore, we find no systematic difference between field strengths on this measure.

Total intracranial volume was determined by tracing the margins of the inner table of the skull on contiguous images of the T_1-weighted spin echo sagittal MR scan (Jack *et al.*, 1989). Raw hippocampal volumes were adjusted for age, gender and total intracranial volume using a *W*-score method (Jack *et al.*, 1997). Hippocampal *W*-scores can be considered age, gender and head size adjusted *Z* scores with 0 mean and 1 SD among normal elderly subjects. Negative *W*-scores, therefore, indicate adjusted volumes below the expected mean for cognitively normal elderly. *W*-scores of −1.65 and 1.65 correspond to the 5th and 95th percentiles in our normal elderly reference population (O'Brien and Dyck, 1995).

Voxel-based morphometry (VBM), within the statistical parametric mapping (SPM5) suite (Ashburner and Friston, 2000), was used to evaluate brain morphometry on a voxel-wise basis. A custom template and tissue probability maps (TPMs) were created in SPM5 using the T_1-weighted 3D MRI scans from all 45 subjects in the study. The custom template and TPMs were created by first normalizing and segmenting the 45 scans using the unified segmentation model in SPM5 with the standard MNI template and TPMs, followed by a clean up step which uses a hidden Markov random field (HMRF) model to increase the accuracy of the individual subject TPMs, and finally averaging the normalized subject TPMs. All subject images were then normalized and segmented using the unified segmentation model and the custom TPMs, followed by the HMRF clean-up step. Jacobian modulation was applied to compensate for the effect of spatial normalization and to restore the original absolute grey matter density in the segmented grey matter images. These modulated images were then smoothed with an 8-mm FWHM smoothing kernel. Grey matter differences between groups were assessed using a two-sided *t*-test within the general linear model framework of SPM.

PiB imaging

Production of PiB and radio labelling with ^{11}C was performed as outlined by Mathis (Mathis *et al.*, 2003). The mean administered activity was 628 MBq (range 385 to 723 MBq). At 25 min, a helical CT image was obtained for attenuation correction. The PET acquisition consisted of 5-min dynamic frames from 40–60 min post-injection. PET sinograms were iteratively reconstructed into a 256-mm FOV. The pixel size was 1.0 mm and the slice thickness 3.3 mm. Individual frames of the PiB dynamic series were realigned if motion was detected and then a mean image was created, referred to from here on as the late uptake image.

PiB image processing and atlas-based brain parcellation for quantitative PiB ROI analysis

The automated anatomic labelling (AAL) atlas (Tzourio-Mazoyer *et al.*, 2002) was modified in-house to contain the following labelled regions of interest (ROI): right and left parietal, temporal, prefrontal, thalamus, striatum, primary sensory-motor, orbito frontal, anterior cingulate, posterior cingulate/precuneus, occipital excluding primary visual and primary visual. The high-resolution T_1 weighted single-subject brain image (Tzourio-Mazoyer *et al.*, 2002) with atlas labels was normalized to the custom template described above in the VBM section using the unified segmentation method in SPM5 (Ashburner, 2005), giving a discrete cosine transformation (DCT), say F, which normalizes the atlas brain to custom template space. The late uptake PiB image volume of each subject was co-registered to his/her own T_1-weighted MRI scan, using a 12-DOF affine registration with mutual information cost function. Each subject MRI scan was then spatially normalized to the custom template using the unified segmentation model of SPM5 (Ashburner, 2005), giving a DCT transformation, say G_i, which normalizes the MRI of subject i to the custom template. Then for each subject, the composite transformation $G_i^{-1}(F(.))$ was applied to the atlas in order to warp the atlas to the subject's native anatomical space. Atlas-based parcellation of PiB images into ROIs was therefore performed in subject space. For each subject, the native-space segmented grey matter probability map generated from the unified segmentation routine was thresholded at a value of 0 to create a binary grey matter mask. Each subject's grey matter mask was then multiplied by the subject-specific warped atlas, to generate a custom grey matter atlas for each subject, parcellated into the aforementioned ROIs. This step was performed in order to minimize inclusion of both CSF and white matter (and thus non-specific white matter PiB retention) in statistics of all ROIs, including the cerebellar ROI, which was used as an input reference (Meltzer, 1999; Sun *et al.*, 2007). Statistics on image voxel values were extracted from each labelled cortical ROI in the atlas. PiB ratio images were calculated by dividing the median value in each target cortical ROI value by the median value in the cerebellar grey matter ROI of the atlas. A global cortical PiB retention summary measure was formed by combining the prefrontal, orbitofrontal, parietal, temporal, anterior cingulate and posterior cingulate/precuneus ratio values for each subject, with equal weighting of the individual values in computing the summary measure.

SPM5 (Ashburner and Friston, 2005) was used to evaluate PiB retention on a voxel-wise basis. Spatial normalization of individual late uptake PiB images to custom template space was performed using the DCT normalization parameters obtained from the co-registered MRI described above. All voxels in the normalized late uptake PiB images were divided by the median PiB uptake of the cerebellar grey matter ROI in each subject to form uptake ratio images. Voxel-wise PiB uptake differences between groups were assessed in SPM5 using a multiple regression model, with indicator vectors to specify diagnostic group and either 'low' or 'high' global PiB retention based on a threshold ratio of 1.5. The rationale for selecting this cut-off value is described in the Results section. Statistical maps displaying group differences were displayed at a significance value of $P<0.01$, corrected for multiple comparisons over the whole brain using the False Discovery Rate correction method (Genovese *et al.*, 2002).

Statistical methods

We compared the proportion of women in each group using a chi-squared test and compared the median age and education across groups using a Kruskal–Wallis test. Differences in performance on the STMS and CDR-SB between the aMCI and AD groups were tested using a two-sided Wilcoxon rank-sum test. Pair-wise group differences on global PiB retention and hippocampal *W*-score are reported as differences in medians with 95% confidence intervals and tested using two-sided Wilcoxon rank-sum tests. These non-parametric methods were used due to skewness in the demographic, functional and imaging measures.

We evaluated the ability of these imaging measures to discriminate between groups by calculating the area under the receiver operating characteristic (ROC) curve and 95% confidence intervals. We summarize how well the imaging variables discriminate or predict among clinical groups using the concordance statistic, a generalization of the area under the ROC curve and R_N^2, a generalization of the coefficient of determination from a linear regression model (Harrell, 2001). The concordance statistic can be interpreted as the proportion of times a pair of randomly selected patients can be correctly ordered on their clinical group using only the predictors in the model while R_N^2 can be interpreted as the proportion of the data log likelihood accounted for by the model relative to a 'perfect fitting' or saturated model, taking into account model complexity.

We estimated the relationship between imaging measures and clinical group using proportional odds logistic regression (POLR) (McCullagh, 1980; Harrell, 2001). POLR is a generalization of binary logistic regression that can be used when there are more than two groups and there is a natural ordering to the groups. In our approach, we assume that on the cognitive impairment spectrum we have the ordering CN < aMCI < AD. Our POLR models have a single coefficient that characterizes the effect of a predictor on the outcome variable. In the models we fit, the coefficients for the imaging predictors represent the log odds of a more impaired diagnosis, in other words the log odds of moving from CN to aMCI or AD, or moving from aMCI to AD. One advantage of having a single coefficient describing the relationship between imaging predictors and clinical group is model parsimony. Another is that the model can be considered as a regression model in which the dependent variable (clinical group) can be interpreted as a discretized or coarsened version of an underlying continuous cognitive impairment spectrum. We fit and report on four POLR models: a model with global cortical PiB retention only, a model with hippocampal *W*-score only, an additive model with both these terms and a model with both terms and an interaction. We compared the predictive ability of models with more versus fewer predictors using likelihood ratio tests.

Results

Demographics

The 20 CN, 17 aMCI and eight AD subjects in this study did not differ significantly on gender, age or education (Table 1). Performance on the STMS and CDR-SB was best in the CN, intermediate in the aMCI and worst in the AD group. Four of the 17 aMCI and seven out of eight AD subjects were being treated with cholinesterase inhibitors. Fourteen of the 17 aMCI subjects were classified as single domain (i.e. memory only impairment), and the remaining three aMCI were multi-domain—i.e. predominate memory impairment with lesser impairments in other domains.

PiB region of interest (ROI) analysis

Right- and left-sided homologous PiB ROI's demonstrated high within subject intra-class correlation, typically above 0.90 and ranging from 0.79 for the temporal ROI to 0.99 for prefrontal. Therefore, the right and left sides were combined for quantitative analyses. Raw cerebellar PiB uptake values on late sum images did not differ by group ($P = 0.46$). This is consistent with the literature and supports use of this ROI as a reference input for normalizing raw cortical PiB retention in this study (Lopresti *et al.*, 2005). Figures 1 and 2 illustrate PiB uptake ratios by group for different ROI's. All ROI's examined except medial temporal were different among the three groups. For data reduction purposes, we combined the six cortical ROIs in Fig. 1 into a global cortical retention ratio value. The rationale for combining these six ROI's into a single global cortical ratio value was several-fold, (i) these cortical areas have been shown on autopsy studies to have high amyloid deposition in AD (Braak and Braak, 1991); (ii) published reports have consistently shown high PiB uptake in these cortical areas (Klunk *et al.*, 2004; Engler *et al.*, 2006; Kemppainen *et al.*, 2006; Mintun *et al.*, 2006; Edison *et al.*, 2007; Forsberg *et al.*, 2007); and (iii) as shown in Supplemental Fig. E1, these six cortical PiB ROI ratios are highly inter-correlated, having an intra-class correlation of 0.91.

Table 2 lists summary global cortical PiB retention ratio, hippocampal volume in cube millimetre and hippocampal volume *W*-score values by clinical group. Box plots with individual data points for all subjects in each of the three clinical groups are illustrated in Fig. 3 for global cortical PiB and hippocampal *W*-score. These plots illustrate that AD subjects are characterized by high PiB and low hippocampal *W*-score; most CN subjects are characterized by low PiB and high hippocampal *W*-score; and group averages for aMCI subjects are intermediate on both PiB and hippocampal *W*-score. However, there are important individual deviations from this pattern. With the exception of one CN subject with an extremely low hippocampal *W*-score (labelled subject B in Figs 3, 5 and 6), the AD and CN hippocampal *W*-score distributions do not overlap; and aMCI subjects are evenly distributed across the AD and CN range. In contrast, while all eight AD subjects are tightly clustered in the high PiB retention range, both the CN and aMCI subjects segregate themselves into high and low PiB

Table 1 Patient characteristics

Characteristic	CN ($n = 20$)	aMCI ($n = 17$)	AD ($n = 8$)	*P*-value
No of women (%)	8 (40.0)	5 (29.4)	5 (62.5)	0.31[a]
Median (range) age, years	76 (72, 90)	79 (56, 87)	70 (54, 91)	0.17[b]
Median (range) education, years	14 (12, 20)	15 (8, 20)	14 (12, 18)	0.84[b]
Median (range) CDR-SB	0 (0, 0.5)	1.5 (0, 4.5)	5.25 (3.5, 9.0)	<0.001[c]
Median (range) MMSE[d]	28 (24, 30)	27 (21, 28)	18 (11, 25)	<0.001[c]

[a]CN vs. aMCI vs. AD using Fisher's exact.
[b]CN vs. aMCI vs. AD using Kruskal–Wallis.
[c]aMCI vs. AD using Wilcoxon rank–sum.
[d]Transformed from the Short Test of Mental Status.

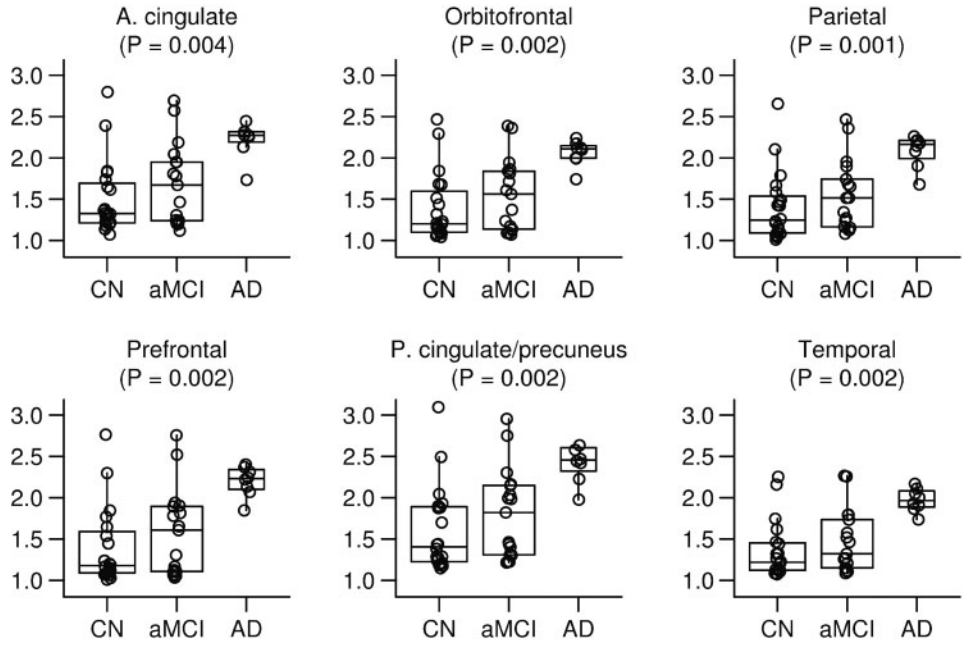

Fig. 1 Regions of interest that constitute the global cortical PiB retention value. Box plots with individual data points superimposed. The horizontal lines in the box plots represent the 25th, 50th and 75th percentiles. The vertical line extending from the box reaches the most extreme data point within 1.5 inter-quartile ranges. Individual data points represent the subject's median target-to-cerebellar ratio over all voxels in the region of interest. The *P*-value shown is based on the three-sample Kruskal–Wallis test.

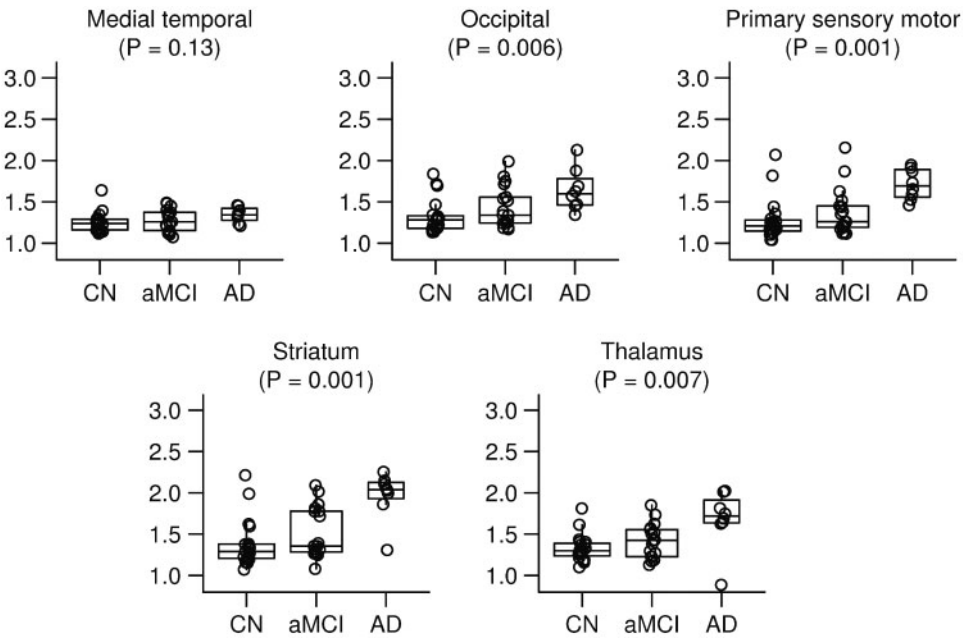

Fig. 2 Regions of interest not part of the global cortical PiB retention value. Box plots with individual data points superimposed. The horizontal lines in the box plots represent the 25th, 50th and 75th percentiles. The vertical line extending from the box reaches the most extreme data point within 1.5 inter-quartile ranges. Individual data points represent the subject's median target-to-cerebellar ratio over all voxels in the region of interest. The *P*-value shown is based on the three-sample Kruskal–Wallis test.

retention groups suggesting bi-modal PiB distribution. Using a ratio of 1.5 as a cut point derived from this data sample, 6 out of 20 CN and 9 out of 17 aMCI subjects can be categorized as high PiB retention subjects. Demographic, imaging and cognitive performance characteristics of CN and aMCI subjects broken out into those with high versus low PiB retention are provided in Table 3. Among CN subjects, those with high PiB retention were slightly older

Table 2 Imaging summary statistics

Imaging measure	CN ($n = 20$)	aMCI ($n = 17$)	AD ($n = 8$)
Global PiB			
Median (IQR)	1.2 (1.1, 1.6)	1.6 (1.1, 1.8)	2.2 (2.1, 2.2)
95% CI for median	1.2 to 1.6	1.3 to 1.8	2.0 to 2.2
Range	1.1 to 2.7	1.1 to 2.5	1.7 to 2.3
Hippocampal volume, mm^3			
Median (IQR)	5401 (4621, 5967)	4685 (4371, 5193)	3912 (3531, 4586)
95% CI for median	4955 to 5731	4412 to 5145	3250 to 4724
Range	3453 to 6813	3895 to 5954	2867 to 4939
Hippocampal W score			
Median (IQR)	0.1 (−0.2, 0.7)	−0.8 (-1.5, 0.1)	−2.6 (−2.6, −2.4)
95% CI for median	−0.2 to 0.7	−1.3 to −0.3	−2.7 to −1.9
Range	−2.6 to 2.0	−2.6 to 0.9	−2.7 to −1.2

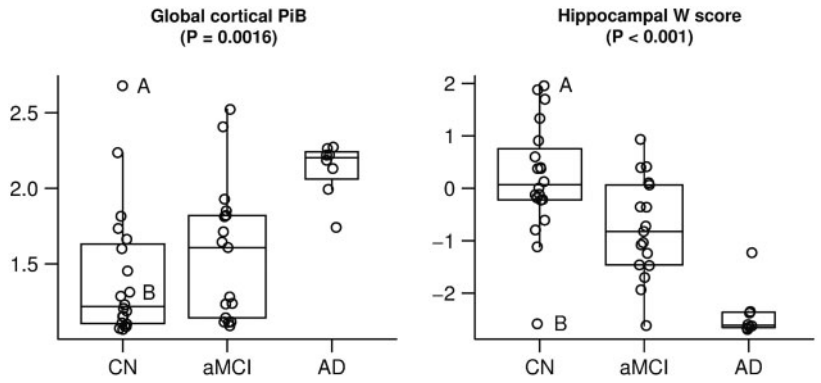

Fig. 3 Group-wise separation for global cortical PiB and hippocampal *W*-score. Box plots with individual data points superimposed. The horizontal lines in the box plots represent the 25th, 50th and 75th percentiles. The vertical line extending from the box reaches the most extreme data point within 1.5 inter-quartile ranges. The *P*-value shown is based on the three-sample Kruskal–Wallis test. The CN subject with the largest PiB value is identified by the letter 'A' and the CN subject with the smallest hippocampal *W*-score is identified by the letter 'B'. These two subjects are described in detail in the text.

and better educated. Overall, there were no consistent differences in cognitive performance between high and low PiB retention CN subjects. High PiB CN subjects performed slightly worse on the WMS-R visual reproduction II and WMS-R logical memory II; the same on AVLT delayed recall, CDR-SB and MMSE*; and better on AVLT sum of learning trials. Among aMCI subjects, those with high PiB retention were slightly younger and better educated. Overall, there were no consistent differences in cognitive performance between high and low PiB retention aMCI subjects. High PiB aMCI subjects performed slightly worse on the WMS-R visual reproduction II and CDR-SB; the same on AVLT delayed recall; and better on AVLT sum of trials, MMSE* and WMS-R logical memory II. The hippocampi were slightly more atrophic in high than low PiB CN and aMCI subjects, although the difference was minimal in aMCI subjects. One could criticize the dichotomization of CN and aMCI subjects into high and low PiB retention groups. However, unlike MRI where all subjects have hippocampi whose volume resides on a continuous scale; the notion that some subjects do and some do not have brain amyloidosis has face validity. The notion of diagnostically positive versus negative PiB scans has been introduced previously (Rabinovici *et al.*, 2007), as has the notion of using a specific cut point to segregate PiB scans into 'AD –like' versus normal (Pike *et al.*, 2007). While the specific cut point of 1.5 may not apply to other samples, dividing subjects into those with and those without cortical PiB retention seems biologically sensible.

Quantitative PiB and MRI comparisons

Representative images of PiB retention ratio by clinical group are found in Fig. 4. The AD subject in Fig. 4 is a 91-year-old woman with a hippocampal *W*-score of –2.6. The CN subject is a 77-year-old man with hippocampal *W*-score of 1.9. The low PiB aMCI subject is an 82-year-old man with hippocampal *W*-score of –1.7. The high PiB aMCI is an 87-year-old woman with hippocampal *W*-score of –0.7. Of interest are two CN subjects with atypical or outlier findings who are labelled subjects A and B in Figs 3, 5 and 6. PiB and MR images of these two atypical CN subjects are illustrated in Fig. 5. Atypical subject A was an 80–year-old

Table 3 Detailed characterization of low and high PiB: CN and aMCI

Characteristic	CN		aMCI	
	PiB ⩽ 1.5	PiB > 1.5	PiB ⩽ 1.5	PiB > 1.5
No of subjects	14	6	8	9
No of women (%)	6 (42.9)	2 (33.3)	1 (12.5)	4 (44.4)
Median (range) age, years	75 (72, 88)	78 (73, 90)	82 (76, 87)	73 (56, 87)
Median (range) education, years	14 (12, 20)	16 (12, 20)	12 (8, 20)	16 (12, 20)
Median (range) MMSE[a]	28 (24, 30)	28 (25, 30)	26 (21, 28)	27 (25, 28)
Median (range) CDR-SB	0 (0, 0.5)	0 (0, 0.5)	1.0 (0, 2.5)	1.5 (0.5, 4.5)
Median (range) AVLT sum of trials	36 (24, 52)	38 (23, 61)	25 (21, 37)	29 (25, 35)
Median (range) AVLT delayed recall	7 (2, 11)	7 (0, 14)	0 (0, 6)	0 (0, 4)
Median (range) WMS-R logical memory II	14 (4, 31)	12 (5, 29)	4 (0, 20)	8 (0, 21)
Median (range) WMS-R visual reproduction II	24 (6, 33)	21 (5, 31)	8 (0, 23)	4 (0, 21)
Median (range) global cortical PiB	1.2 (1.1, 1.5)	1.8 (1.6, 2.7)	1.1 (1.1, 1.3)	1.8 (1.6, 2.5)
Median (range) hippocampal W score	0.3 (-2.6, 1.9)	−0.1 (−1.1, 2.0)	−0.7 (-1.9, 0.9)	-0.8 (−2.6, 0.4)

Maximum scores: CDR-SB, 18; MMSE, 30; AVLT sum, 75; AVLT delayed recall, 15; WMS-R logical memory II, 50; WMS-R visual reproduction II, 41.
[a]Transformed from the Short Test of Mental Status

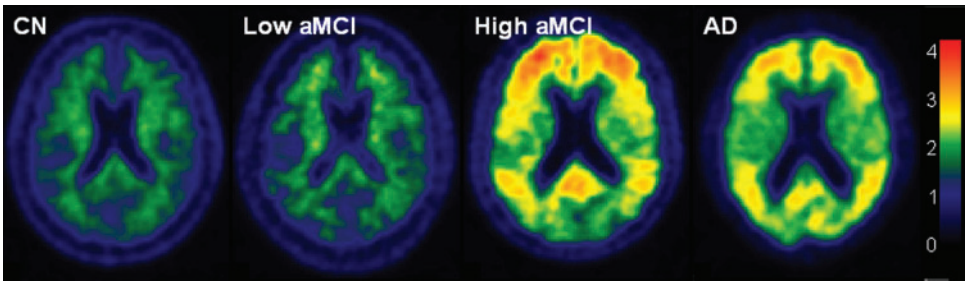

Fig. 4 Typical PiB subjects. The colour scale bar represents cortical voxel-to-cerebellar retention ratio.

woman with the highest global cortical PiB retention ratio (2.7) in the study but who had a hippocampal *W*-score of 2.0 (i.e. non-atrophic) and was cognitively normal with MMSE*, 29; CDR-SB, 0.0; AVLT sum of trials, 53; AVLT delayed recall, 14 (the highest value in the study); WMS-R logical memory II, 19 and WMS-R visual reproduction II, 22. Atypical subject B had an extremely low hippocampal *W*-score (–2.6) but had a low global cortical PiB retention ratio (1.3) and, while performing worse cognitively than atypical subject A, was also cognitively normal with MMSE*, 28; CDR-SB, 0.0; AVLT sum of trials, 30; AVLT delayed recall, 6; WMS-R logical memory II, 13 and WMS-R visual reproduction II, 11.

We correlated global cortical PiB retention ratio and hippocampal *W*-score (separately) with the WMS-R visual reproduction II, WMS-R logical memory II, AVLT delayed recall, AVLT sum of learning trials, CDR-SB and MMSE* across all 45 subjects in the study. The imaging–cognitive correlations went in the expected directions and were significant at the 0.05 or greater level, except correlations between PiB and AVLT sum of learning trials ($P = 0.08$) and PiB and MMSE* ($P = 0.09$) which neared significance. The magnitudes of the correlations were greater for hippocampal *W*-score than global cortical PiB retention (Table 4). One could criticize our approach of using *W*-score scaling of hippocampal volumes with no similar scaling of PiB data; the *W*-score scales for inter-subject variation in head size, gender and age. It is difficult to envision a scenario where PiB retention ratios reliably scale with the first two variables. And without a great deal of additional PiB data in cognitively normal elderly (which is not available yet), it is not clear how one would appropriately scale PiB retention for age.

For each of three pair-wise diagnostic comparisons—CN versus aMCI, CN versus AD and aMCI versus AD—the ability of the global cortical PiB retention ratio and hippocampal *W*-score to effect group-wise separation was highly significant (Table 5), with the exception of CN versus aMCI discrimination by PiB ($P = 0.17$). Figure 6 is a scatter plot of global PiB versus hippocampal *W*-score with each subject in the study identified by clinical group membership. While the two modalities are negatively correlated (Spearman's rho = –0.48, $P < 0.001$) there is considerable scatter of individual points, suggesting that the two modalities do not contain entirely overlapping diagnostic information. Supplemental Table E1 is a numeric representation of the values in the quadrants of Fig. 6 by clinical group.

To evaluate the complementary diagnostic nature of PiB and hippocampal volume further, we used ordinal logistic

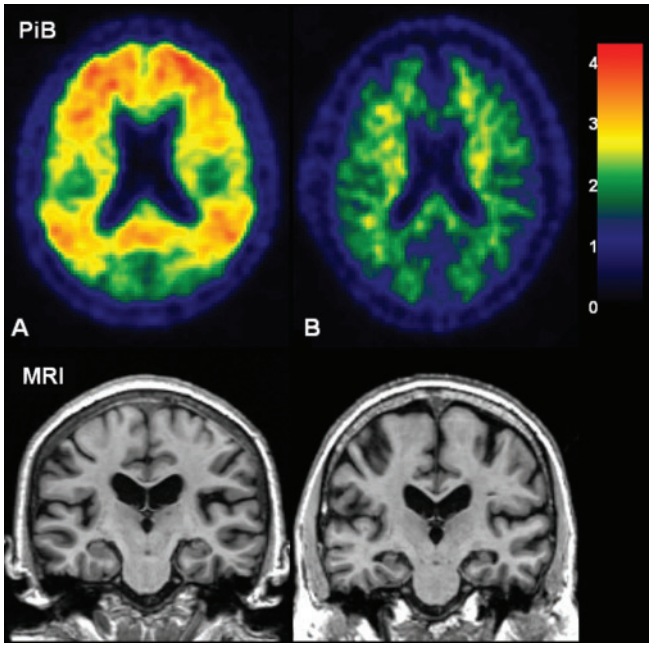

Fig. 5 Atypical findings in CN subjects. Subject A has the highest global PiB cortical retention ratio in the study but an above average hippocampal *W*-score and normal cognitive function. Subject B has a low hippocampal *W*-score but low PiB retention and normal cognitive function. The colour scale bar represents cortical voxel-to-cerebellar retention ratio.

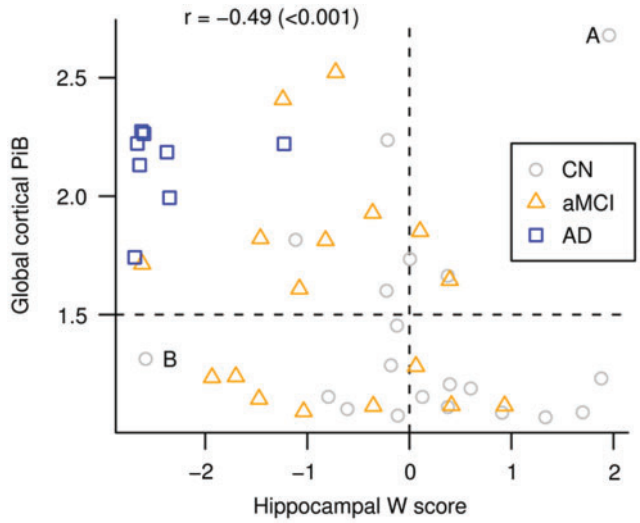

Fig. 6 Scatter plot showing relationship between global cortical PiB retention and hippocampal *W*-score. Spearman rank correlation (*P*-value) indicated in the top left. Reference lines at a *W*-score of zero and a global cortical PiB of 1.5 have been added to the plot to segregate the data into quadrants. The CN subject with the largest PiB value is identified by the letter 'A' and the CN subject with the smallest hippocampal *W*-score is identified by the letter 'B'.

regression models to assess the ability of global cortical PiB retention and hippocampal *W*-score alone and in combination to diagnostically discriminate among members of the three patient groups. The results are presented in Table 6

Table 4 Pair-wise Spearman rank correlation (*P*-value) between imaging and clinical functional measures among all subjects

	Global cortical PiB	Hippocampal W score
CDR-SB	0.54 (<0.001)	−0.71 (<0.001)
MMSE[a]	−0.25 (0.09)	0.44 (0.002)
AVLT sum of trials	−0.27 (0.08)	0.51 (<0.001)
AVLT delayed recall	−0.34 (0.03)	0.47 (0.002)
WMS-R logical memory II	−0.36 (0.02)	0.40 (0.01)
WMS-R visual reproduction II	−0.34 (0.03)	0.56 (<0.001)

[a]Transformed from the Short Test of Mental Status

and can be summarized as follows. Global PiB ($P<0.001$) and hippocampal *W*-score ($P<0.001$) were each separately found to be significantly associated with clinical diagnosis. When a model is fit including both these predictors, both the hippocampal *W*-score ($P<0.001$) and the global PiB term ($P=0.04$) remain significant.

There is evidence of an interaction between global PiB and hippocampal volume ($P=0.009$). Interpretation of the interaction model can be simplified by considering four possible scenarios: (i) for subjects with a low hippocampal *W*-score, defined as the 25th percentile, there was strong evidence of increasing odds of a more-impaired diagnosis as PiB retention increases from the 25th to the 75th percentile (OR 23, 95% CI 2.2 to 229). This can be envisioned as moving vertically from the lower left to the upper left quadrant of Fig. 6; (ii) for subjects with a high hippocampal *W*-score, defined as at the 75th percentile, there is no significant increase in the odds of a more-impaired diagnosis as PiB retention increases from the 25th to the 75th percentile (OR 0.66, 95% CI 0.08 to 5.2). This can be envisioned as moving vertically from the lower right to the upper right quadrant of Fig. 6; (iii) for subjects with a low PiB retention ratio, defined as the 25th percentile, the odds of a more-impaired diagnosis do not increase significantly for a subject with a hippocampal *W*-score at the 25th percentile versus one at the 75th percentile (OR 2.8, 95% CI 0.54 to 14). This can be envisioned as moving horizontally from the lower right to the lower left quadrant of Fig. 6; and (iv) for a subject with a high PiB retention ratio, defined as the 75th percentile, the odds of a more-impaired diagnosis increase precipitously as hippocampal *W*-score decreases from the 75th percentile to the 25th percentile (OR 95, 95% CI 6.9 to 1316). This can be envisioned as moving horizontally from the upper right to the upper left quadrant of Fig. 6.

Voxel-wise PiB and MRI analyses

We wished to compare the topographical distribution of PiB uptake and grey matter loss in subjects who occupied opposite poles of the clinical diagnostic continuum (CN and AD)

Table 5 Paired group-wise differences for imaging measures

Marker	CN vs. aMCI	CN vs. AD	aMCI vs. AD
Global PiB			
P-value[a]	0.17	<0.001	0.004
Difference in medians (95% CI)	−0.39 (−0.51 to 0.05)	−0.99 (−1.06 to −0.53)	−0.59 (−0.99 to −0.32)
AUC (95% CI)	0.64 (0.45 to 0.82)	0.91 (0.79 to 1.00)	0.85 (0.69 to 1.00)
Hippocampalvolume W score			
P-value[a]	0.009	<0.001	<0.001
Difference in medians (95% CI)	0.89 (0.25 to 1.62)	2.68 (2.06 to 3.11)	1.79 (0.94 to 2.41)
AUC (95% CI)	0.75 (0.59 to 0.91)	0.98 (0.94 to 1.00)	0.93 (0.83 to 1.00)

AUC = area under the receiver operating characteristic (ROC) curve.
[a]Two-sided, two-sample Wilcoxon rank-sum test.

Table 6 Summaries of performance of proportional odds ordinal logistic regression models

Model	Likelihoodratio chi-squared (*P*-value)[a]	Concordance/ generalized AUC[b]	Generalized R^{2c}
Global cortical PiB only	12.2 (<0.0001)	0.75	0.27
Hippocampal W score only	29.2 (<0.0001)	0.84	0.55
Global PiB and W score[d]	33.4 (<0.0001)	0.86	0.60

Due to skewness, global PiB was log transformed.
[a]Likelihood ratio test versus the null model.
[b]This can be interpreted as the probability of correctly identifying which is the more clinically impaired patient from a pair of patients having different diagnoses using only the imaging measure(s) in the model.
[c]This can be interpreted as the model likelihood divided by the likelihood from a saturated, or 'perfect fitting' model, after adjusting for model complexity. In some sense, what proportion of the observed data is 'explained' by the model.
[d]Significantly better than PiB only model ($P < 0.001$) and hippocampal W score only model ($P = 0.040$) by likelihood ratio test.

using voxel-wise methods. We performed an SPM analysis of PiB uptake in all AD versus all CN subjects, corrected for multiple comparisons (false discovery rate, FDR) and thresholded at $P < 0.01$ (Fig. 7). We also performed a VBM analysis of grey matter loss between all AD and all CN subjects, uncorrected for multiple comparisons and thresholded at $P < 0.01$ (Fig.7). PiB uptake in AD was significantly greater than CN subjects in prefrontal, lateral temporal, lateral parietal and posterior cingulate/precuneus regions. No significant differences in PiB uptake between AD and CN were found in the primary sensorimotor areas, visual cortex or anteromedial temporal lobe. In contrast, grey matter loss in AD relative to CN subjects was significant in the lateral temporoparietal cortex, basal temporal and medial temporal lobe.

In Fig. 8, we present a voxel-wise conjunction analysis (Nichols *et al.*, 2005) of PiB cortical-to-cerebellar retention ratio, corrected for multiple comparisons (FDR) and thresholded at $P < 0.01$. Our objective was to identify those areas in the brain where the topographical distribution of PiB was similar among all subjects who did display PiB retention—i.e. AD, high PiB CN and high PiB aMCI. We took the PiB distribution in low PiB CN subjects as an appropriate topographical representation of little or no PiB retention. The figure illustrates all voxels where PiB retention in AD > low PiB CN, 'and' high PiB aMCI > low PiB CN 'and' high PiB CN > low PiB CN. As illustrated in Fig. 8, the set of voxels which meet the above criteria are located in the medial and lateral prefrontal, anterior and posterior cingulate/precuneus and lateral temporal and parietal cortical areas.

Discussion

Major conclusions from this study fall into three different categories: group-wise diagnostic separation by PiB and MRI, correlations between imaging and cognitive performance and conclusions related to the topographical distribution of amyloid deposition and grey matter tissue loss in subjects lying along the cognitive continuum from CN to aMCI to AD. Comparison of the topographical distribution of cerebral grey matter loss and amyloid deposition in subjects with AD versus CN (Fig. 7) reveals both areas of concordance and discordance between the two pathological processes associated with AD. Both grey matter loss and amyloid deposition were observed in the lateral temporal and parietal association cortices. Although the posterior cingulate/precuneus was not significant in our VBM comparison of grey matter loss between AD and CN, we attribute this to the small number of AD subjects in our study because this area has been found to be significant in other VBM studies with larger sample sizes (Rombouts *et al.*, 2000; Baron *et al.*, 2001; Chetelat *et al.*, 2002; Frisoni *et al.*, 2002; Senjem *et al.*, 2005; Whitwell *et al.*, 2007*a*, *b*). Neither amyloid deposition nor cerebral grey matter loss was present in the primary visual and sensorimotor cortices. There were also areas of the brain where intermodality discordance was observed. In the frontal lobes, extensive PiB retention was observed in AD; however, grey matter loss was negligible. In the anteromedial temporal

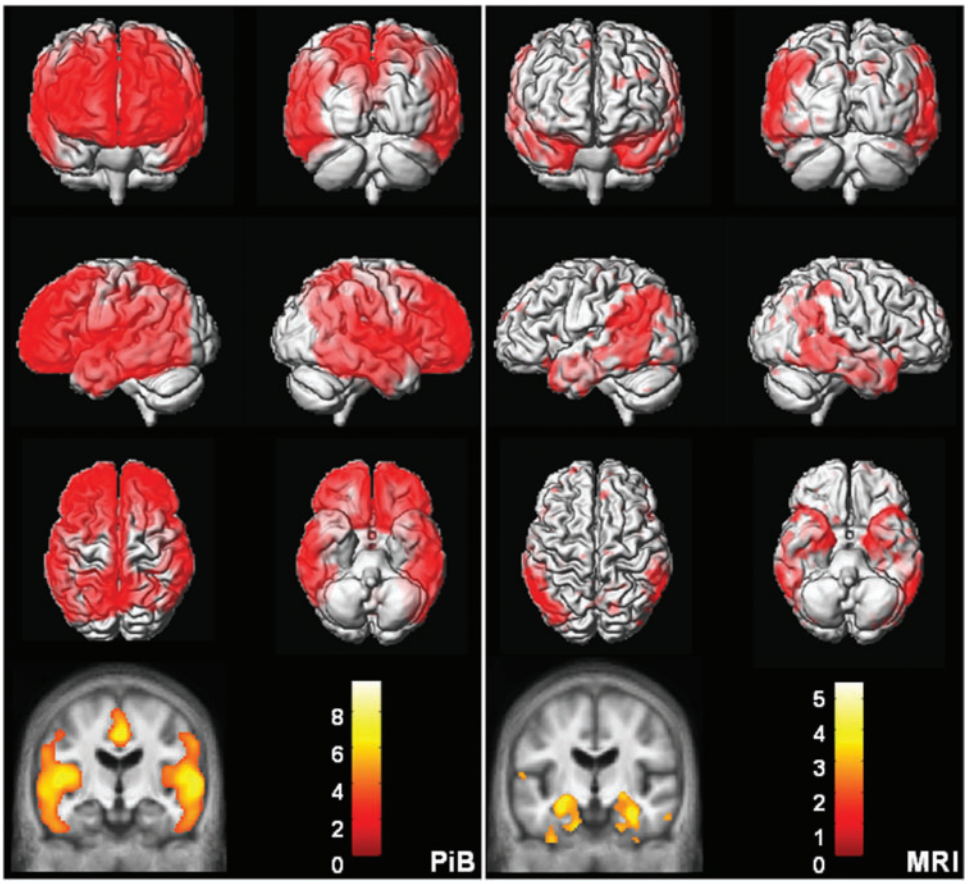

Fig. 7 AD versus CN voxel mapping. PiB (left): SPM of PiB retention ratio. Corrected for multiple comparisons (FDR) and thresholded at $P < 0.01$. MRI (right): VBM of MRI grey matter density. Uncorrected for multiple comparisons and thresholded at $P < 0.01$. The colour bar values indicate the value of the *T*-statistic in each display.

lobe, extensive grey matter loss was seen in AD, whereas PiB retention was negligible.

Comparison of the topographical distribution of findings in PiB and MRI support the notion that different brain regions have intrinsically different susceptibilities to different pathological expressions of AD. The posterior cingulate/precuneus, and lateral temporoparietal association cortex seem to be susceptible to both plaque deposition and grey matter loss. Primary visual and sensorimotor cortical areas are susceptible to neither. The prefrontal cortex is susceptible to plaque deposition but not to grey matter loss. The medial and basal temporal lobe are highly susceptible to grey matter loss but not to plaque deposition. Similar findings of topographical concordance/discordance have also been observed when FDG-PET measures of regional glucose uptake are compared with PiB (Engler *et al.*, 2006; Edison *et al.*, 2007; Forsberg *et al.*, 2007). Blomquist *et al.* (2005) have shown that PiB binding does not appear to be affected by variation in cerebral perfusion. Moreover, while we found some areas where PiB retention is low and atrophy is present (i.e. medial temporal lobe), we found other areas where both are present (i.e. temporal-partial association cortex). Therefore, decreased cerebral blood flow and therefore ^{11}C PiB delivery is an unlikely explanation for low amyloid deposition in areas of atrophy.

One could criticize the fact that we did not correct for multiple comparisons in the MRI VBM analysis (Fig. 7), and also the fact that we compared two SPM maps in the same subjects (Fig. 7) that were thresholded with different statistical criteria. The counter argument to that criticism is that comparing 'increases' in PiB retention and 'decreases' in grey matter density are not straightforward. The two pathologies (amyloid deposition and grey matter loss) are quite different. Fibrillar amyloid deposits are not present in the cortex of the majority of CN subjects whereas grey matter is present in all subjects. Moreover, while not correcting the VBM analysis for multiple comparisons can be criticized, the fact is that the resulting map comparing grey matter loss between AD and CN matches the known topographical distribution of neurofibrillary pathology and also matches the topographical distribution of grey matter loss in published VBM studies comparing AD versus CN with larger samples of subjects (Braak and Braak, 1991; Rombouts *et al.*, 2000; Baron *et al.*, 2001; Chetelat *et al.*, 2002; Frisoni *et al.*, 2002; Senjem *et al.*, 2005; Whitwell *et al.*, 2007*a*, *b*). Therefore, the VBM map in Fig. 7 while

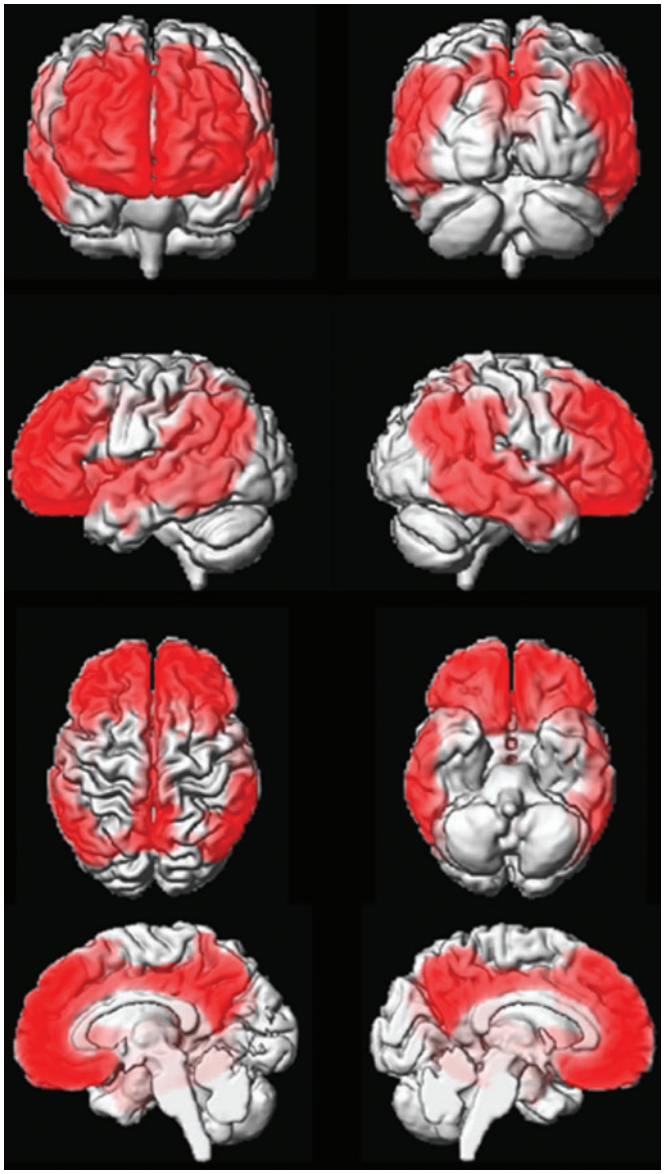

Fig. 8 PiB conjunction analysis. The figure illustrates all voxels where PiB retention in AD > low PiB CN, 'and' high PiB aMCI > low PiB CN 'and' high PiB CN > low PiB CN. Corrected for multiple comparisons (FDR) and thresholded at $P < 0.01$.

not corrected for multiple comparisons does have face validity both in terms of consistency with prior literature and concordance with known biology of AD.

The SPM conjunction analysis in Fig. 8 illustrates the common topographical distribution of voxels in subjects with cortical PiB retention (AD, high PiB CN and high PiB aMCI) compared to the low PiB CN group. The set of voxels which meet the above criteria are located in the medial and lateral prefrontal, anterior and posterior cingulate/precuneus and lateral temporal and parietal cortical areas. This closely matches the expected distribution of fibrillar amyloid plaques from AD pathological studies and also matches the distribution of PiB retention in AD subjects from published PiB studies (Arnold *et al.*, 1991; Braak and Braak, 1991; Thal *et al.*, 2002; Klunk *et al.*, 2004; Engler *et al.*, 2006; Kemppainen *et al.*, 2006; Mintun *et al.*, 2006; Edison *et al.*, 2007; Forsberg *et al.*, 2007; Rowe *et al.*, 2007). Figure 8 illustrates a common topographical distribution of PiB retention across subjects of widely varying cognitive status—the high PiB CN group is cognitively normal, the high PiB aMCI group is mildly impaired and the high PiB AD group is demented. In fact, the subject with the highest levels of PiB uptake in our study was a CN subject who was cognitively completely intact (atypical subject A in Figs 3, 5 and 6), and in fact has an AVLT delayed recall score (14) as high as any subject in the study.

One way to explain this apparent dissociation between current cognitive performance and PiB retention in some CN subjects is to propose that amyloid deposition is an early event in the disease process ultimately leading to clinical AD. Others have proposed that high levels of amyloid and hence PiB retention are established in the clinically pre-symptomatic phase of AD (Engler *et al.*, 2006; Mintun *et al.*, 2006). Based on this proposed sequence of events, the findings illustrated in Fig. 8 are logical, with the high PiB retention CN subjects representing individuals with high brain amyloid levels who are in the presymptomatic phase of the disease. Studies of plaque biology (Hyman *et al.*, 1993; Christie *et al.*, 2001) also suggest that amyloid deposition is an early event that reaches a state of dynamic balance. Once this state of dynamic balance is reached, while individual plaques may appear and disappear, overall plaque burden reaches a plateau. Longitudinal MRI studies have shown that brain atrophy precedes, by at least several years, declining cognitive performance in subjects who later progress to AD (Fox *et al.*, 1996, 2001; Kaye *et al.*, 1997; Jack *et al.*, 1999, 2005; Visser *et al.*, 1999 Killiany *et al.*, 2002). A possible sequence of events that integrates PiB, MRI and clinical findings is that amyloid deposition is an antecedent event that precedes clinical symptoms by many years. Neuronal pathology appears later and heralds impending cognitive decline. With the appearance of cognitive symptoms, the brain continues to atrophy on MRI while the patient declines clinically, but PiB retention remains relatively constant at a plateau level. In support of this proposed sequence of events, we found that the six high PiB retention and 14 low PiB retention CN subjects were very similar cognitively, the hippocampus on average was slightly, albeit not significantly, more atrophic in the high PiB than the low PiB CN subgroup, and the PiB uptake between subgroups was clearly separable (by definition). This is clearly a hypothesis and it will require longitudinal multi-modality studies for support.

A subtle but important point about the 'PiB remains stable once amyloid load is established' hypothesis is that it does not imply that PiB deposition at the present time is not correlated with cognition at the present time. Rather, we believe that high PiB deposition today that has been present for a period of time (arbitrarily say 10 or more

years) will likely be associated with impairment today, whereas high PiB deposition that has only been in place a short time will not be associated with dementia today. Our hypothesis is that amyloid deposition (i.e. high PiB retention) alone is not sufficient to cause dementia in many (most?) elderly subjects. Additional pathological event(s) must take place once PiB is deposited before cognitive impairment is seen. One of these events is neuronal damage which can be detected as grey matter loss by MRI. This is consistent with the idea that amyloid deposition is an antecedent event—i.e. it occurs before cognitive changes are evident. Our results and hence conclusions differ from those recently published by Pike *et al.* (2007) who found poorer performance on memory tests in high PiB versus low PiB controls. In contrast, we found no consistent differences in detailed learning and memory performance between high and low PiB CN subjects. How often subjects may have significant amyloid deposition and still be cognitively intact is of great interest and will undoubtedly be the focus of future studies.

Correlations between imaging and functional performance across all subjects follow expected patterns with high PiB retention and greater hippocampal atrophy (i.e. more negative hippocampal *W*-scores) associated with worse cognitive and functional performance (Table 3). In our sample, the magnitudes of the correlations between cognitive performance and hippocampal *W*-score were greater than those seen between global PiB retention and cognitive performance. Investigators who have evaluated PiB and FDG-PET in the same subjects have observed a similar phenomenon, with FDG-PET generally showing better correlation with current cognitive performance than PiB, with the presumption that FDG-PET, like MRI, is closely linked to neuronal health (Engler *et al.*, 2006; Edison *et al.*, 2007). Because PiB deposition is bi-modal within the CN and aMCI groups, correlations between cognition and PiB are to a great extent simply a reflection of the proportions within each clinical group who are PiB positive versus PiB negative.

About half of the aMCI subjects in this study fall into the high PiB uptake range (global cortical-to-cerebellar retention ratio > 1.5), and half fall into the low PiB retention range. While the proportion of PiB negative aMCI subjects in our study may be higher than seen in other studies, perhaps due to the older ages in our study, observing PiB negative aMCI subjects is consistent with results from other studies (Lopresti *et al.*, 2005; Price *et al.*, 2005; Pike *et al.*, 2007; Rowe *et al.*, 2007). Interestingly, as with our CN subjects, no consistent differences in cognitive performance including learning and memory were seen between high versus low PiB aMCI subjects. The upper left and lower right quadrants in Fig. 6 represent concordant PiB and MRI findings (i.e. high PiB and low hippocampal *W*-score, or vice versa), while the lower left and upper right panels represent subjects with discordant PiB and MRI findings. Of the 17 aMCI subjects in the study, PiB and MRI were discordant in seven. Five of these seven had low PiB retention and hippocampal *W*-scores <0. A hypothesis is that low PiB retention aMCI subjects who also have atrophic hippocampi have prodromal dementias other than AD, and at autopsy will be found to have pathological substrates for their cognitive impairment other than AD, for example hippocampal sclerosis, cerebrovascular disease or non-AD neurodegenerative conditions. Conversely, we suspect that aMCI subjects who lie in the high PiB retention range have prodromal AD, which will be confirmed at autopsy. However, this is purely a hypothesis and longitudinal studies to autopsy are required to confirm or refute this. The implication of our findings for the concept of aMCI is that this syndrome represents prodromal AD in some but not all those affected. This result is completely consistent with the original formulation of the construct of aMCI as a risk factor for AD, not a diagnosis of early AD (Petersen, 1995; Petersen *et al.*, 1995). Although one can reasonably infer that PiB positive aMCI subjects have prodromal AD and will progress to clinical AD with time, the same is not true of PiB negative aMCI subjects. PiB negative aMCI subjects therefore constitute a very interesting group and longitudinal follow-up is necessary in order to determine the outcome of these subjects.

The numbers of subjects in this study are too small to pursue a rigorous evaluation of diagnostic, sensitivity and specificity. Nonetheless, it is clear that overall the ability to separate aMCI from AD, and CN from AD is not dramatically different between standard hippocampal volume measures and global cortical measures of PiB retention. Pair-wise inter-group discrimination was significant for all measures except for control versus aMCI with PiB ($P = 0.17$). This is not surprising given the distribution of PiB retention values in the CN and aMCI subjects in Fig. 3 which illustrates that while sample medians were found to differ, high and low PiB retention subjects exist in both the CN and aMCI clinical groups.

Table 5 illustrates that across all three clinical groups, diagnostic inter-group separation appears to be slightly better by MRI than PiB. These results on inter-group diagnostic separation as well as correlation of imaging with functional measures present an apparent paradox given the fact that PiB retention is a direct measure of a pathological process that is central to AD, whereas MRI is an indirect measure of synapse and neuron loss which is not specific for AD. A way to resolve this apparent paradox is to consider the likely timing of events in the pathogenesis of AD. As outlined above, if PiB deposition plateaus prior to the first appearance of clinical symptoms, whereas MRI becomes abnormal shortly before the appearance of clinical symptoms and then declines in parallel with clinical decline, then it is not surprising that MRI measures seem to correlate slightly better with current clinical diagnostic status than PiB retention measures. From the initial report, it has been pointed out that PiB is a tool to detect brain β-amyloidosis, not dementia *per se* (Klunk *et al.*, 2004). The potential clinical use of PiB is not likely to be the

separation of cognitively normal controls from MCI or AD patients. Amyloid imaging will more likely be used in the context of ruling in or ruling out AD from the differential diagnosis of a subject with a clinical dementia that does not fall easily into any one diagnostic category.

The evidence presented in this paper implies that the diagnostic information contained in PiB and that contained in structural MRI is complementary in predicting clinical group membership. While hippocampal volumes may be a slightly stronger predictor of group membership, PiB adds independent diagnostic information to hippocampal volumes and hippocampal volumes add independent predictive information to PiB. This complimentary relationship as quantified in the interaction POLR model suggests a natural interpretation: smaller hippocampal volumes and higher PiB retention are much riskier for more-impaired clinical diagnosis than either of these traits alone. This is also supported graphically in Fig. 6, which shows that all demented subjects have both elevated global PiB retention and reduced hippocampal *W*-scores. The interaction model also provides some evidence that the absence of hippocampal atrophy is somewhat protective, regardless of the subject's PiB levels.

Emerging evidence from longitudinal clinical studies with autopsy endpoints supports the notion that cognitive performance in life depends on the sum of various pathological insults to the brain which increase in prevalence with age. Cognitive performance is not completely explained by pathological assessments of the burden of any single pathology, but rather by the overall multi-factorial pathology burden in each individual (Green *et al.*, 2000; Snowdon *et al.*, 1997; Troncoso *et al.*, 1996; White *et al.*, 2005). Results presented in this study support this notion. The fact that structural MRI measures of hippocampal neuronal damage and PiB PET measures of amyloid burden better discriminate among, and are more predictive of, clinical groups than either measure alone support the idea that both of these pathological insults, which can be detected *in vivo* by imaging, contribute to the observed cognitive performance levels in individual subjects. This concept can be extended to include other imaging modalities, each capable of providing an *in vivo* window into a specific type of pathological disturbance affecting individuals along the CN to aMCI to AD continuum.

The complementary nature of different imaging modalities can be further extended to the area of predicting future cognitive course in individual subjects. It may be that the ability of one imaging modality to predict future cognitive course will be superior at one point in the disease while a different modality will be superior at a different point in the disease. For example, current expectation is that PiB is an accurate marker of fibrillar amyloid in the brain and that a positive PiB study in a clinically asymptomatic subject indicates a high likelihood that the subject will develop clinical AD if he/she lives long enough. Conversely, MRI might be a better predictor of future cognitive course once a subject has reached a plateau of fibrillar amyloid deposition. These are clearly hypotheses however and the studies required to test these hypotheses remain to be done.

The notion that that MRI and PiB provide complementary information extends to the SPM/VBM analyses—where clear and meaningful differences in topographical distribution exist between the two modalities. These imaging findings have significant implications for formulation of mechanistic theories in AD. These results imply that the full expression of AD pathology in humans is not fully captured by a single pathway that is applicable throughout the brain, typically beginning with disordered amyloid metabolism or clearance and leading to plaque formation and neuronal damage. Rather, the expression of different aspects of AD pathology varies topographically and a unifying theory of cause and effect at the molecular level must accommodate this topographical variation.

Supplementary material

Supplementary material is available at *Brain* online.

Acknowledgements

The authors thank Denise Reyes, Peter O'Brien, PhD, Scott Przybelski, Jennifer Whitwell, PhD and Kejal Kantarci, MD for assistance with data and manuscript preparation. This study was supported by National Institute on Aging [P50 AG16574, U01 AG06786, C06 RR018898, and R01 AG11378]; the Robert H. and Clarice Smith and Abigail Van Buren Alzheimer Disease Research Program; and the Alexander Family Alzheimer's Disease Research Professorship of the Mayo Foundation, U.S.A. Funding to pay the Open Access publication charges for this article was provided by the National Institute on Aging (NIH AG11378).

References

Diagnostic and statistical manual of mental disorders, DSM-IV. Washington, D.C.: American Psychiatric Association, 1994.

Archer H, Edison P, Brooks DJ, Barnes J, Frost C, Yeatman T, et al. Amyloid load and cerebral atrophy in Alzheimer's disease: an 11C-PIB positron emission tomography study. Ann Neurol 2006; 60: 145–7.

Arnold SE, Hyman BT, Flory J, Damasio AR, et al. The topographical and neuroanatomical distribution of neurofibrillary tangles and neuritic plaques in the cerebral cortex of patients with Alzheimer's disease. Cerebral Cortex 1991; 1: 103–16.

Ashburner J, Friston KJ. Voxel-based morphometry–the methods. Neuroimage 2000; 11: 805–21.

Ashburner J, Friston KJ. Unified Segmentation. Neruoimage 2005; 26: 839–851.

Bacskai BJ, Frosch MP, Freeman SH, Raymond SB, Augustinack JC, Johnson KA, et al., Molecular imaging with Pittsburgh Compound B confirmed at autopsy: a case report. Arch Neurol 2007; 64: 431–4. doi:10.1001/archneur.64.3.431.

Baron JC, Chetelat G, Desgranges B, Perchey G, Landeau B, de la Sayette V, et al. In vivo mapping of gray matter loss with voxel-based morphometry in mild Alzheimer's disease. Neuroimage 2001; 14: 298–309.

Blomquist G, Ringheim A, Extrada S, Hoglund U, Frandberg P, Nylen G. Influx and net accumulation of PIB compared with CBF in a rhesus monkey. EJNM 2005; 32: S263.

Bobinski M, de Leon MJ, Wegiel J, Desanti S, Convit A, Saint Louis LA, et al. The histological validation of post mortem magnetic resonance imaging-determined hippocampal volume in Alzheimer's disease. Neuroscience 2000; 95: 721–5.

Braak H, Braak E. Neuropathological staging of Alzheimer-related changes. Acta Neuropathol 1991; 82: 239–59.

Buckner RL, Snyder AZ, Shannon BJ, LaRossa G, Sachs R, Fotenos AF, et al. Molecular, structural, and functional characterization of Alzheimer's disease: evidence for a relationship between default activity, amyloid, and memory. J Neurosci 2005; 25: 7709–17.

Chetelat G, Desgranges B, de la Sayette V, Viader F, Eustache F, Baron C-J. Mapping gray matter loss with voxel-based morphometry in mild cognitive impairment. Brain Imaging 2002; 13: 1939.

Christie RH, Bacskai BJ, Zipfel WR, Williams RM, Kajdasz ST, Webb WW, et al. Growth arrest of individual senile plques in a model of Alzheimer's disease observed by in vivo multiphoton microscopy. J Neurosci 2001; 21: 858–64.

Crystal H, Dickson D, Sliwinski M, Lipton R, Grober E, Marks-Nelson H, et al. Pathological markers associated with normal aging and dementia in the elderly. Ann Neurol 1993; 34: 566–73.

Csernansky JG, Hamstra J, Wang L, McKeel D, Price JL, Gado MH, et al. Correlations between antemortem hippocampal volume and postmortem neuropathology in AD subject. Alzheimer Dis Assoc Disord 2004; 18: 190–5.

de Leon MJ, George AE, Stylopoulos LA, Smith G, Miller DC. Early marker for Alzheimer's disease: the atrophic hippocampus. Lancet 1989; 2: 672–3.

Edison P, Archer HA, Hinz R, Hammers A, Pavese N, Tai YF, et al. Amyloid, hypometabolism, and cognition in Alzheimer disease: An [11C]PIB and [18F]FDG PET study. Neurology 2007; 68: 501–8. doi:10.1212/01.wnl.0000244749.20056.d4.

Engler H, Forsberg A, Almkvist O, Blomquist G, Larsson E, Savitcheva I, et al. Two-year follow-up of amyloid deposition in patients with Alzheimer's disease. Brain 2006; 129: 2856–66. doi:10.1093/brain/awl178.

Fagan AM, Mintun MA, Mach RH, Lee SY, Dence CS, Shah AR, et al. Inverse relation between in vivo amyloid imaging load and cerebrospinal fluid Abeta42 in humans. Ann Neurol 2006; 59: 512–9.

Folstein MF, Folstein SE, McHugh PR. ''Mini Mental State': a practical method for grading the cognitive state of patients for the clinician. J Psychiatr Res 1975; 12: 189–98.

Forsberg A, Engler H, Almkvist O, Blomquist G, Hagman G, Wall A, et al. PET imaging of amyloid deposition in patients with mild cognitive impairment. Neurobiol Aging 2007, in press.

Fox NC, Crum WR, Scahill RI, Stevens JM, Janssen JC, Rossor MN. Imaging of onset and progression of Alzheimer's disease with voxel-compression mapping of serial magnetic resonance images. Lancet 2001; 358: 201–5.

Fox NC, Warrington EK, Freeborough PA, Hartikainen P, Kennedy AM, Stevens JM, et al. Presymptomatic hippocampal atrophy in Alzheimer's disease. A longitudinal MRI study. Brain 1996; 119: 2001–7.

Frisoni GB, Testa C, Zorzan A, Sabattoli F, Beltramello A, Soininen H, et al. Detection of gray matter loss in mild Alzheimer's disese with voxel-based morphometry. J Neurol Neurosurg Psychiatry 2002; 73: 657–64.

Genovese CR, Lazar NA, Nichols TE. Thresholding of statistical maps in functional neuroimaging using the false discovery rate. Neuroimage 2002; 15: 772–86.

Gosche KM, Mortimer JA, Smith CD, Markesbery WR, Snowdon DA. Hippocampal volume as an index of Alzheimer neuropathology: findings from the Nun Study. Neurology 2002; 58: 1476–82.

Green M, Kaye JA, Ball MJ. The Oregon Brain Aging Study. Neurology 2000; 54: 105–13.

Harrell FE. Regression modeling strategies: with applications to linear models, logistic regression, and survival analysis. New York: Springer-Verlag; 2001; 1–568.

Hulette CM, Welsh-Bohmer KA. Neuropathological and neuropsychological changes in ''normal'' aging: evidence for preclinical Alzheimer disease in cognitively normal individuals. J Neuropathol Exp Neurol 1998; 57: 1168–74.

Hyman B, Marzloff K, Arriagada PV. The lack of accumulation of senile plaques or amyloid burden in Alzheimer's disease suggests a dynamic balance between amyloid deposition and resolution. J Neuropathol Exp Neurol 1993; 52: 594–600.

Jack CR Jr, Bernstein MA, Fox NC, Thompson P, Alexander GE, Harvey D, et al. The Alzheimer's Disease Neuroimaging Initiative (ADNI): MRI methods. JMRI 2007, in press.

Jack CR Jr, Petersen RC, O'Brien PC. MR-based hippocampal volumetry in the diagnosis of Alzheimer's disease. Neurology 1992; 42: 183–8.

Jack CR Jr, Petersen RC, Xu Y, O'Brien PC, Smith GE, Ivnik RJ, et al. Prediction of AD with MRI-based hippocampal volume in mild cognitive impairment. Neurology 1999; 52: 1397–403.

Jack CR Jr, Petersen RC, Xu Y, O'Brien PC, Smith GE, Ivnik RJ, et al. The rate of medial temporal lobe atrophy in typical aging and Alzheimer's disease. Neurology 1998; 51: 993–9.

Jack CR Jr, Petersen RC, Xu YC, Waring SC, O'Brien PC, Tangalos EG, et al. Medial temporal atrophy on MRI in normal aging and very mild Alzheimer's disease. Neurology 1997; 49: 786–94.

Jack CR Jr, Shiung MM, Weignad SD, O'Brien PC, Gunter JL, Boever BF, et al. Brain atrophy rates predict subsequent clinical conversion in normal elderly and amnestic MCI. Neurology 2005; 65: 1227–31.

Jack CR Jr, Twomey CK, Zinsmeister AR, Sharbrough FW, Petersen RC, Cascino GD. Anterior temporal lobes and hippocampal formations: normative volumetric measurements for MR images in young adults. Radiology 1989; 172: 549–54.

Jack CR Jr, Dickson DW, Parisi JE, Xu YC, Cha RH, O'Brien PC, et al. Antemortem MRI findings correlate with hippocampal neuropathology in typical aging and dementia. Neurology 2002; 58: 750–7.

Katzman R, Terry R, DeTeresa R, Brown T, Davies P, Fuld P, et al. Clinical, pathological, and neurochemical changes in dementia: a subgroup with preserved mental status and numerous neocortical plaques. Ann Neurol 1988; 23: 138–441.

Kaye JA, Swihart T, Howieson D, Dame A. Volume loss of the hippocampus and temporal lobe in healthy elderly persons destined to develop dementia. Neurology 1997; 48: 1297–04.

Kemppainen NM, Aalto S, Wilson IA, Nagren K, Helin S, Bruck A, et al. Voxel-based analysis of PET amyloid ligand [11C]PIB uptake in Alzheimer disease. Neurology 2006; 67: 1575–80. doi:10.1212/01.wnl.0000240117.55680.0a.

Kemppainen NM, Aalto S, Wilson IA, Nagren K, Helin S, Bruck A, et al. PET amyloid ligand [11C]PIB uptake is increased in mild cognitive impairment. Neurology 2007; 68: 1603–6. doi:10.1212/01.wnl.0000260969.94695.56.

Killiany RJ, Hyman BT, Gomez-Isla T, Moss MB, Kikinis R, Jolesz F, et al. MRI measures of entorhinal cortex vs hippocampus in preclinical AD. Neurology 2002; 58: 1188–96.

Kinniany RJ, Moss MB, Albert MS, Sandor T, Tieman J, Jolesz F. Temporal lobe regions on magnetic resonance imaging identify patients with early Alzheimer's disease. Arch Neurol 1993; 50: 949–54.

Klunk WE, Engler H, Nordberg A, Wang Y, G B, P HD, et al. Imaging brain amyloid in Alzheimer's disease with Pittsburgh Compound-B. Ann Neurol 2004; 55: 306–19.

Knopman DS, Parisi JE, Salviati A. Neuropathology of cognitively normal elderly. J Neuropathol Exp Neurol 2003; 62: 1087–95.

Kokmen E, Smith GE, Petersen RC, Tangalos E, Ivnik RC. The short test of mental status: correlations with standardized psychometric testing. Arch Neurol 1991; 48: 725–8.

Laakso MP, Soininen H, Partanen K, Lehtovirta M, Hallikainen M, Hanninen T, et al. MRI of the hippocampus in Alzheimer's disease:

sensitivity, specificity, and analysis of the incorrectly classified subjects. Neurobiol Aging 1998; 19: 23–31.

Lopresti BJ, Klunk WE, CMathis CA, Hoge JA, Ziolko SK, Lu X, et al. Simplified quantification of Pittsburgh compound B amyloid imaging PET studies: a comparative analysis. J Nucl Med 2005; 46: 1959–72.

Mathis CA, Wang Y, Holt DP, Huang GF, Debnath ML, Klunk WE. Synthesis and evaluation of 11C-labeled 6-substituted 2-arylbenzothiazoles as amyloid imaging agents. J Med Chem 2003; 46: 2740–54.

McCullagh P. Regression models for ordinal data. J R Stat S Ser B (Methodol) 1980; 42: 109–42.

McKhann G, Drachman D, Folstein M, Katzman R, Price D, Stadlan EM. Clinical diagnosis of Alzheimer's disease: report of the NINCDS-ADRDA work group under the auspices of Department of Health and Human Services Task Force on Alzheimer's disease. Neurology 1984; 34: 939–44.

Meltzer C, Kinahan PE, Greer PJ, Nichols TE, Comtat C, Cantwell MN, et al. Comparative evaluation of MR-based partial-volume correction schemes for PET. J Nucl Med 1999; 40: 2053–65.

Mintun MA, LaRossa GN, Sheline YI, Dence CS, Lee SY, Mach RH, et al. [11C]PIB in a nondemented population: Potential antecedent marker of Alzheimer disease. Neurology 2006; 67: 446–52. doi:10.1212/01.wnl.0000228230.26044.a4.

Morris J, Price J. Pathologic correlates of nondemented aging, mild cognitive impairment, and early-stage Alzheimer's Disease. J Mol Neurosci 2001; 17: 101–18.

Morris JC. The Clinical Dementia Rating (CDR): current version and scoring rules. Neurology 1993; 43: 2412–14.

Nichols TE, Brett M, Andersson JLR, Wager T, Poline J-B. Valid conjunction inference with the minimum statistic. Neuroimage 2005; 25: 653–60.

O'Brien PC, Dyck PJ. Procedures for setting normal values. Neurology 1995; 45: 17–23.

Petersen RC. Normal aging, mild cognitive impairment, and early Alzheimer's disease. The Neurologist 1995; 1: 326–344.

Petersen RC, Doody RS, Kurz A, Hohs R, Morris JC, Rabins PV, et al. Current concepts in mild cognitive impairment. Arch Neurol 2001; 58: 1985–92.

Petersen RC, Kokmen E, Tangalos E, Ivnik RJ, Kurland LT. Mayo Clinic Alzheimer's Disease Patient Registry. Aging 1990; 2: 408–415.

Petersen RC, Smith GE, Ivnik RJ, Tangalos EG, Schaid DJ, Thibodeau SN, et al. Apolipoprotein E status as a predictor of the development of Alzheimer's disease in memory impaired individuals. JAMA 1995; 273: 1274–78.

Pike KE, Savage G, Villemagne VL, Ng S, Moss SA, Maruff P, et al. Beta-amyloid imaging and memory in non-demented individuals: evidence for preclinical Alzheimer's disease. Brain 2007; 130: 2837–44.

Price JC, Klunk WE, Lopristi BJ, Lu X, Hoge JA, Ziolko SK, et al. Kinetic modeling of amyloid binding in humans using PET imaging and Pittsburgh Compound-B. J Cereb Blood Flow Metab 2005; 25: 1528–47.

Price JL, Morris JC. Tangles and plaques in nondemented aging and "preclinical" Alzheimer's disease. Ann Neurol 1999; 45: 358–68.

Rabinovici GD, Furst AJ, O'Neil JP, Racine CA, Mormino EC, Baker SL, et al. 11C-PIB PET imaging in Alzheimer disease and frontotemporal lobar degeneration. Neurology 2007; 68: 1205–12. doi:10.1212/01.wnl.0000259035.98480.ed.

Rey A.2 L'examen clinique en psychologie. Paris: Presses Universitaires de Frances; 1964; 1–221.

Riley KP, Snowdon DA, Markesbery WR. Alzheimer's neurofibrillary pathology and the spectrum of cognitive function: findigns from the Nun Study. Ann Neurol 2002; 51: 567–77.

Rombouts SA, Barkhof F, Witter MP, Scheltens P. Unbiased whole-brain analysis of gray matter loss in Alzheimer's disease. Neurosci Lett 2000; 285: 231–3.

Rowe CC, Ng S, Ackermann U, Gong SJ, Pike K, Savage G, et al. Imaging {beta}-amyloid burden in aging and dementia. Neurology 2007; 68: 1718–25. doi:10.1212/01.wnl.0000261919.22630.ea.

Schmitt FA, Davis DG, Wekstein D. "Preclinical" AD revisted: neuropathology of cognitively normal older adults. Neurology 2000; 55: 370–6.

Senjem ML, Gunter JL, Shiung MM, Petersen RC, Jack CR Jr. Comparison of different methodological implementations of voxel-based morphometry in neurodegenerative disease. Neuroimage 2005; 26: 600–8.

Silbert LC, Quinn JF, Moore MM, Corbridge E, Ball MJ, Murdoch G, et al. Changes in premorbid brain volume predict Alzheimer's disease pathology. Neurology 2003; 61: 487–92.

Small GW, Kepe V, Ercoli LM, Siddarth P, Bookheimer SY, Miller KJ, et al. PET of brain amyloid and Tau in mild cognitive impairment. N Engl J Med 2006; 355: 2652–63.

Snowdon DA, Greiner LH, Mortimer JA, Riley KP, Greiner PA, Markesbery WR. Brain infarction and the clinical expression of Alzheimer's disease, The Nun Study. JAMA 1997; 277: 813–7.

Sun FT, Schriber RA, Greenia JM, He J, Gitcho A, Jagust WJ. Automated templeate-based PET region of interest analyses in the aging brain. Neuroimage 2007; 34: 608–17.

Tang-Wai DF, Knopman DS, Geda YE, Edland SD, Smith GE, Ivnik RJ, et al. Comparison of Short Test of Mental Status and Mini Mental State Examination in mild cognitive impairment. Arch Neurol 2003; 60: 1777–81.

Terry RD, Masliah E, Salmon DP, Butters N, DeTeresa R, Hill R, et al. Physical basis of cognitive alterations in Alzheimer's disease: synapse loss is the major correlate of cognitive impairment. Ann Neurol 1991; 30: 572–80.

Thal DR, Rub U, Orantes M, Braak H. Phases of Ab-deposition in the human brain and its relevance for the development of AS. Neurology 2002; 58: 1791–800.

Troncoso JC, Martin LJ, Del Forno G, Kawas CH. Neuropathology in controls and demented subjects from the Baltimore Longitudinal Study of Aging. Neurobiol Aging 1996; 17: 365–71.

Tzourio-Mazoyer N, Landeau B, Papathanassiou D, Crivello F, Etard O, Delcroix N, et al. Automated anatomical labeling of activations in SPM using a macroscopic anatomical parcellation of the MNI MRI single-subject brain. Neuroimage 2002; 15: 273–89.

Verhoeff NP, Wilson AA, Takeshita S, Trop L, Hussey D, Singh K, et al. In-vivo imaging of Alzheimer disese beta=amyloid with (11C)SB-13 PET. Am J Geriatr Psychiatry 2004; 12: 584–95.

Visser PJ, Scheltens P, Verhey FRJ, Schmand B, Launer LJ, Jolles J, et al. Medial temporal lobe atrophy and memory dysfunction as predictors for dementia in subjects with mild cognitive impairment. J Neurol 1999; 246: 477–85.

Wechsler D. Wechsler Memory Scale-Revised. New York, NY: Psychological Corp, Harcourt Brace Janvanovich, Inc.; 1987.

White L, Small BJ, Petrovitch H, Ross GW, Masaki K, Abbott RD, et al. Recent clinical-pathologic research on the causes of dementia in late life: update from the Honolulu-Asia Aging Study. J Geriatr Psychiatr Neurol 2005; 18: 224–7.

Whitwell JL, Shiung MM, Przybelski SA, Weigand SD, Knopman DS, Boeve BF, et al. MRI patterns of atrophy associated with progression to AD in amnestic mild cognitive impairment. Neurology 2007a; in press.

Whitwell JL, Weigand SD, Shiung MM, F BB, Ferman TJ, Smith GE, et al. Focal atrophy in dementia with Lewy bodies on MRI: a distinct pattern from Alzheimer's disease. Brain 2007b; 130: 708–19.

Zarow C, Vinters HV, Ellis WG, Weiner MW, Mungas D, White L, et al. Correlates of hippocampal neuron number in Alzheimer's disease and ischemic vascular dementia. Ann Neurol 2005; 57: 896–903.